Barrier heights and electrical properties of intimate metal-AlGaAs junctions

M. Eizenberg,[a] M. Heiblum, M. I. Nathan, N. Braslau, and P. M. Mooney
IBM Thomas J. Watson Research Center, Yorktown Heights, New York 10598

(Received 28 August 1986; accepted for publication 29 October 1986)

The dependence of the Schottky barrier height of Mo-*n*:AlGaAs junctions, fabricated *in situ* by molecular beam epitaxy, on the Al mole fraction (x) was determined by internal photoemission measurements and by activation energy plots of the current versus voltage dependence on temperature. Both techniques yielded similar values. The difference in barrier height of Mo-AlGaAs as a function of x, compared to that of Mo-GaAs, was found to be equal to the conduction band discontinuity in AlGaAs-GaAs heterojunctions for Al concentrations in the range $0 \leqslant x \leqslant 0.4$. For $x > 0.4$, values of the barrier heights were somewhat lower than values of the band discontinuity; however, both dependencies on x were quite similar. The temperature dependence of the current-voltage characteristics showed that thermionic emission was the dominant transport mechanism at forward bias for temperatures higher than 250 K. At lower temperatures, current transport was governed by thermionic field emission.

I. INTRODUCTION

$Al_xGa_{1-x}As$ layers are an integral part of many of the most advanced GaAs high speed devices. For example, in modulation-doped field effect transistors (MODFET), the metal-AlGaAs Schottky contact plays a crucial role. Therefore, attention should be paid to the interfaces of these ternary alloys with metals.

Aside from the technological importance, the dependence of the Schottky barrier height on the Al mole fraction (x), is also of scientific interest. The electronic structure of metal-semiconductor interfaces, in general, is still not well understood. This is revealed by the large number of models suggested to explain the Fermi level position in the junction interface, which includes Schottky's work function model,[1] the modified work function model of Freeouf and Woodall,[2] Bardeen's surface state role,[3] metal induced gap states,[4,5] and Spicer's native defects model.[6] A systematic study of the dependence of the Schottky barrier height on the Al mole fraction can contribute to the testing of some of the suggested models, since by varying x one can compare many different diodes, all prepared in a similar way, using the same metal, and with the semiconductors having similar lattice parameters and only slightly different band structures.

However, the available experimental results for Schottky barrier heights on AlGaAs substrates are scarce. Best[7] reported on measurements done on junctions consisting of Au films deposited on n-type AlGaAs epilayers grown by liquid phase epitaxy, where an unavoidable native oxide layer existed at the metal-semiconductor interface. The barrier height, ϕ_b^n, was found to increase up to $x \sim 0.4$, followed by a decrease for higher x. The inferred barrier height on p-type ($\phi_b^p = E_g - \phi_b^n$, where E_g is the energy gap) increased linearly from $x = 0$ to $x = 1$. In a later report by Okamoto *et al.*,[8] an intimate Al contact was formed *in situ* to AlGaAs grown by molecular beam epitaxy (MBE). Different values of ϕ_b^n were obtained as growth conditions varied, most probably due to the strong reactivity of Al with the AlGaAs; however, the same general trend found by Best was also observed. Since the above sets of measurements were carried out on nonideal structures, a more detailed study of nearly ideal junctions is necessary. This will allow a comparison of the barrier heights for different x with the conduction band discontinuity, ΔE_c, in AlGaAs-GaAs heterojunctions, and will enable us to check a recently suggested correlation between ΔE_c and $\Delta\phi_b^n = \phi_b^n(\text{Mo-AlGaAs}) - \phi_b^n(\text{Mo-GaAs})$.[9-11]

The mechanism for transport of carriers across the Schottky barrier and its dependence on the Al mole fraction have not been studied in detail. Even in the simpler case of $x = 0$ (metal-GaAs) nonideal behavior (deviations from thermionic emission) was observed in the current-voltage characteristics.[12] Thus, the second goal of the present work was to learn about the transport mechanism of carriers by studying the current-voltage-temperature (I-V-T) characteristics. Molybdenum was chosen as the contacting metal with the AlGaAs since no metal-semiconductor chemical interactions take place in the range of temperatures employed.[13] Special care was exercised to ensure extremely clean and oxide-free junctions by making all layers, including the metal in a molecular beam epitaxy (MBE) system, without breaking the vacuum.

The procedures for the layer's growth and the processing of the diodes are described in Sec. II. The study of the Schottky barrier height dependence on x is described in Sec. III; the measurements of ϕ_b^n by the internal photoemission (IPE) technique and by activation energy plots of the current-voltage dependence on temperature are presented in Sec. III A, whereas the correlation between the determined barrier heights dependence on x with the conduction band discontinuity in AlGaAs-GaAs heterojunctions, ΔE_c, is discussed in Sec. III B. The study of the transport of carriers across the Schottky barrier is described in Sec. IV; the I-V-T characteristics and the suggested carrier transport mechanisms are described and discussed in Sec. IV A, while the measurements of electron traps in the AlGaAs and their ef-

[a] Permanent address: Dept. of Materials Engineering and the Solid State Institute, Technion-Israel Institute of Technology, Haifa 32000, Israel.

 0021-8979/87/041516-07$02.40

fects on the I-V characteristics are presented in Sec. IV B. The study is summarized in Sec. V.

II. EXPERIMENTAL PROCEDURES

Intimate junctions without interfacial oxide were obtained by the growth of the semiconductor layers followed by deposition of the metal layer in an MBE system. The nominal background pressures during these evaporations were 5×10^{-11} and 3×10^{-10} Torr, respectively. The structures were grown on n^+ (1×10^{18} cm^{-3} Si doped) (100) GaAs substrates after a thorough precleaning and *in situ* outgassing. A 1-μm-thick GaAs buffer layer doped with Si to $\sim10^{18}$ cm^{-3} was grown first (at a substrate temperature of 600 °C), followed by a 1000-Å-thick graded region to $Al_xGa_{1-x}As$. In this region, the Al flux was gradually increased to give the desired alloy composition, while the Si flux was gradually decreased to yield a doping of 5×10^{16}–1.5×10^{17} cm^{-3}, and the substrate temperature was raised to 700 °C. This graded region was followed by a $\sim$5000-Å-thick layer of Si-doped $Al_xGa_{1-x}As$. Special care was exercised to leave the top surface of the AlGaAs with the same reconstruction after each growth, and to maintain it up to the onset of the metal deposition. When the As background was reduced to $\sim2\times10^{-10}$ Torr, a thin ($\sim$200 Å thick) Mo layer was then deposited *in situ* at a substrate temperature of $\sim$200 °C, using a 5-kW electron gun evaporator specially designed to minimize the escape of stray electrons,[14] thus maintaining a very low pressure during evaporation.

Each sample was analyzed for the Al mole fraction by microprobe (with a relative accuracy of $\pm$ 5%), and for the AlGaAs net doping concentration by capacitance-voltage measurements. The latter were carried out both in the dark at room temperature, and under illumination at 77 K. Good agreement was obtained between these two sets of measurements.

Diodes were prepared by etching 0.5×0.5 and 0.25×0.25 mm^2 mesas to a depth of $\sim1\,\mu$m. Gold dots were evaporated at the corner of each square to facilitate top contact to the thin Mo layer. Standard NiAuGe ohmic contacts were formed on the back side of the samples.

III. SCHOTTKY BARRIER HEIGHT DEPENDENCE ON Al MOLE FRACTION

A. Barrier height determination

The Schottky barrier heights for the Mo-AlGaAs system as a function of x were determined by two techniques: (1) internal photoemission (IPE) and (2) activation energy plots of the current-voltage dependence on temperature. Both techniques and their results are described below.

1. Internal photoemission measurements

The internal photoemission experiment provides a direct measurement of the Schottky barrier height with no adjustable parameters. In this method, the yield Y (photocurrent per absorbed photon), which results from electrons that are excited in the metal and surmount the barrier ϕ_b^n entering the semiconductor, is given by[15]

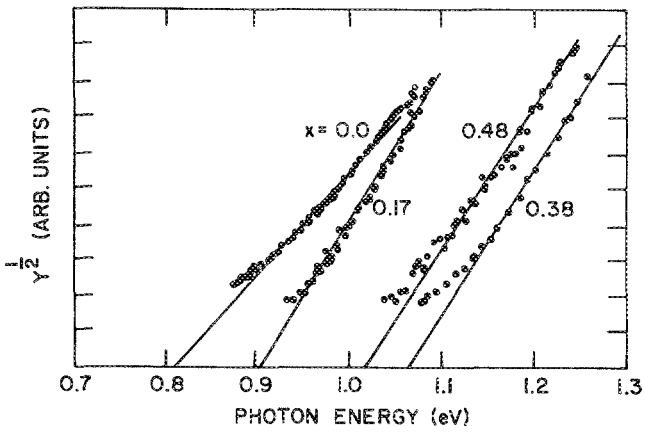

FIG. 1. Photoresponse curves of the IPE experiment in Schottky barriers shown with $x = 0, 0.17, 0.38, 0.48$. Currents are in the picoamperes range.

$$Y = C\,(h\nu - \phi_b^n)^2, \tag{1}$$

for $h\nu > \phi_b^n + 3kT$. Here, $h\nu$ is the photon energy, k is Boltzmann's constant, T the absolute temperature, and C is a constant. The short circuit photocurrent was measured at 300 K as a function of the photon energy at zero applied bias. Illumination by a quartz tungsten lamp was done through the thin Mo layer. A grating monochromator was used for wavelength selection, and a lock-in technique with computer averaging was employed. Figure 1 shows a few photoresponse curves; the extrapolation of the linear regime to zero photocurrent yields the barrier height. Image force corrections estimated as 30 meV for our doping levels were added to the measured values. The resulting accuracy in ϕ_b^n was estimated as $\pm$ 20 meV. The resultant barrier heights for nine different Al mole fractions are presented in Fig. 2 (de-

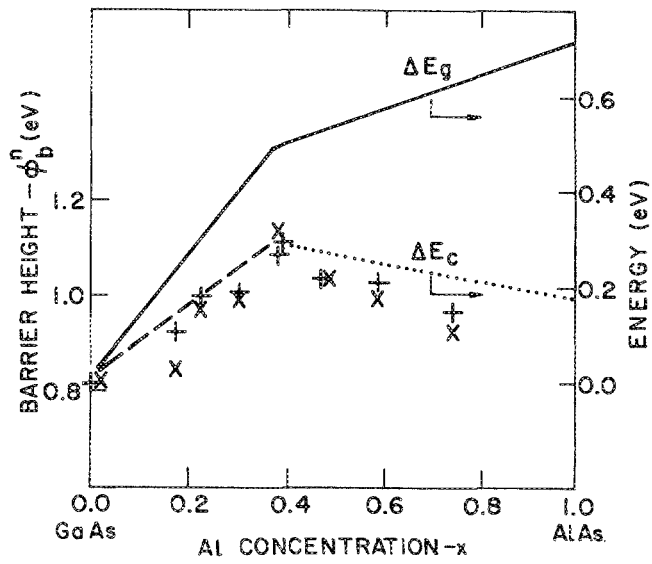

FIG. 2. Schottky barrier heights of Mo-AlGaAs diodes measured by IPE (marked by +) and measured by the activation energy method (marked by ×), as a function of Al mole fraction. The conduction band discontinuity ΔE_c, for GaAs-AlGaAs heterojunctions with $x < 0.4$ measured by IPE (Ref. 18) is given by the broken line; ΔE_c for $x > 0.4$ inferred from the results of Ref. 19 is given by the dotted line. The band-gap difference (ΔE_g) according to Ref. 16 is given by the solid line.

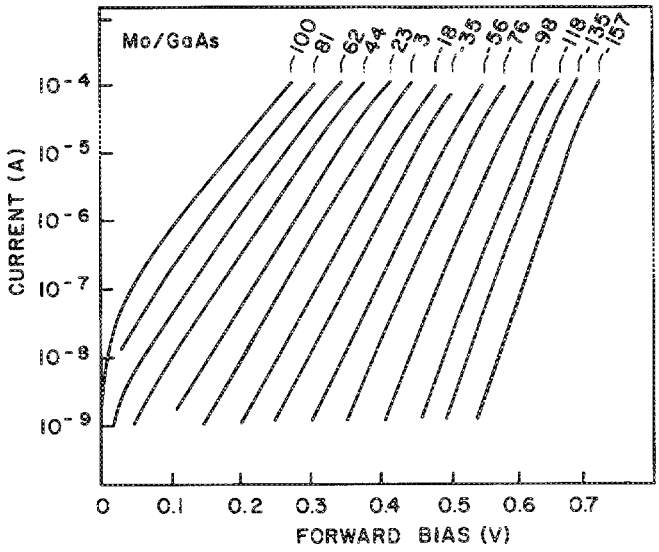

FIG. 3. Current-voltage characteristics for Mo-GaAs Schottky barriers shown under forward bias for temperatures in the range − 157 to 100 °C.

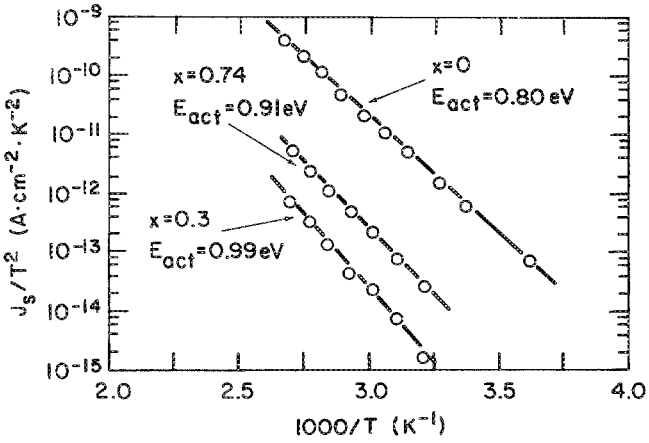

FIG. 4. Richardson plots shown to determine activation energy for a few Schottky diodes with different Al mole fractions ($x = 0$, 0.3, 0.74). The current density values used are those found by extrapolating the current values to zero bias.

noted by +). As x increases, the Schottky barrier height increases up to 1.12 eV at $x = 0.39$; thereafter the Schottky barrier decreases gradually.

2. Activation energy measurements

It has been shown that for Schottky barriers formed on several lightly doped wide band-gap semiconductors, such as GaAs, current transport at forward bias V at 300 K is governed by thermionic emission, and the current density J is given by[17]

$$J = J_s[\exp(qV/nkT) - 1], \qquad (2)$$

$$\sim J_s \exp(qV/nkT) \quad \text{for } V > 3kT/q,$$

where J_s is the extrapolated current density to zero bias and is equal to $A^* T^2 \exp(q\phi_b^n/kT)$, n is a number close to unity and is called the ideality factor, A^* is the effective Richardson constant, and q is the electron charge.

Current-voltage measurements were performed in the temperature range 77–380 K. A typical result for $x = 0$ is presented in Fig. 3. For a given x, the current values of different diodes were found to scale with their areas, resulting in area independent values of J. Richardson plots[15] of $\log J_s/T^2$ vs $1/T$, for different x, were then plotted, as seen in Fig. 4. The straight lines show that the current transport was via thermionic emission in the high temperature range ($T \geqslant 250$ K in most cases). The slope of each straight line curve yields the activation energy, E_{act}, which for zero bias is the Schottky barrier height. The resultant barrier heights (including the above mentioned image force correction) for different values of x are shown in Fig. 2 (marked by ×); good agreement with the results of the internal photemission technique was obtained. Similar values for ϕ_b^n were also inferred from measuring E_{act} at a forward bias V, using $\phi_b^n = E_{act} + V$. The fact that the electrical measurements support the internal photoemission results is important since, although there are no adjustable parameters in the latter technique, one must choose correctly the range of photon energy for extrapolation to ϕ_b^n from Eq. (1). The spectrum must show the characteristic saturation for $h\nu - \phi < 3kT$ and the spectral region of excess current due to band-to-band processes as $h\nu$ approaches E_g is excluded.

B. The correlation between $\Delta\phi_b^n$ and ΔE_c

The composition dependence of $\Delta\phi_b^n$ is different from that of the energy gap, $\Delta E_g = E_g\ (Al_x Ga_{1-x} As) - E_g$ (GaAs).[16] The latter is given by the solid curve in Fig. 2. However, the x dependence of $\Delta\phi_b^n$ agrees well with that of ΔE_c (the conduction band discontinuity across the AlGaAs-GaAs heterointerface). The dependence of ΔE_c on x up to $x = 0.4$ (the composition at which the energies of the X and Γ valleys of the AlGaAs become equal, thus changing the band structure from direct to indirect) has been recently determined by several techniques.[17] The broken line in Fig. 2 represents our recent results for ΔE_c, determined by a similar internal photoemission technique employed on Mo-GaAs-AlGaAs structures,[18] which conform to many other recent works.[17] The agreement between $\Delta\phi_b^n$ and ΔE_c in the direct regime ($x \leqslant 0.4$) is very good. The dotted line in Fig. 2 represents ΔE_c, for $x > 0.4$, inferred from the values of ΔE_v measured recently by Batey and Wright[19] ($\Delta E_c = \Delta E_g - \Delta E_v$). $\Delta\phi_b^n$ is somewhat lower than ΔE_c in this regime; the determination of ΔE_g vs x (Ref. 16) could be responsible, in part, for this discrepancy.

A correlation between semiconductor heterojunction band discontinuities and metal-semiconductor Schottky barrier heights has only recently been proposed.[9–11] Katnani and Margaritondo[9] have pointed out that Spicer's defect model[6] for Schottky barrier formation can be applied to heterojunctions where the Fermi level is pinned, thus accounting for the band discontinuities. However, since in GaAs-AlGaAs heterojunctions the number of interface states is very small,[20] this model is ruled out. More recently, Tersoff has suggested[10] that band alignments at metal–semiconductor and semiconductor–semiconductor interfaces are controlled by an interfacial dipole, which is induced by tunneling of bulk electrons from one material into the band gap of the other. In this model, the level at which energy states

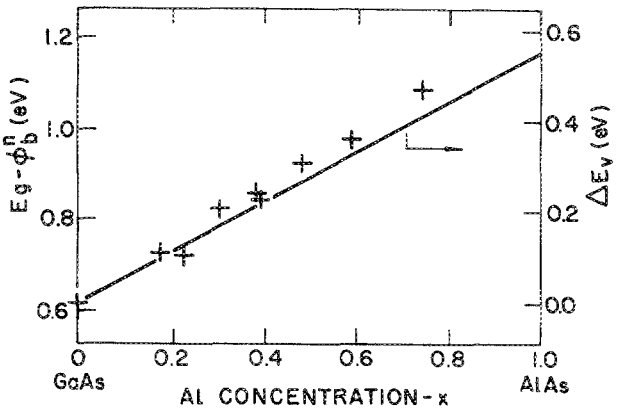

FIG. 5. Deduced barrier height to p-type AlGaAs $\phi_b^p = E_g - \phi_b^n$ as a function of Al mole fraction. The valence band discontinuity according to Ref. 19 is given by the solid line.

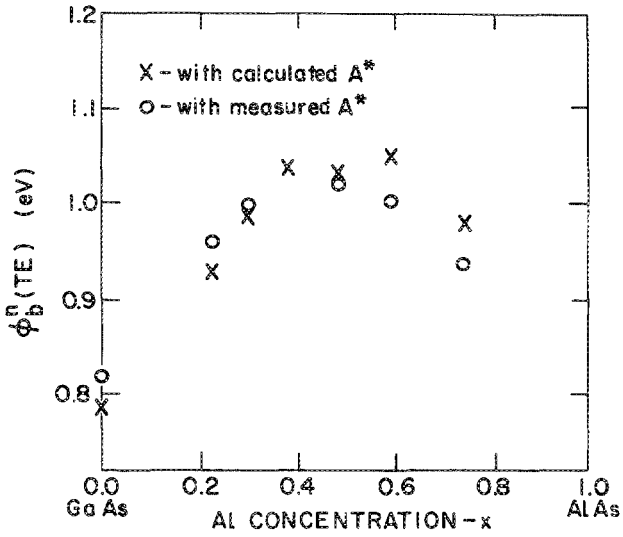

FIG. 6. Dependence on Al mole fraction of the barrier height at 300 K calculated according to Eq. (2). A^* values used are according to calculation (corresponding barriers marked by x), and according to extrapolation of Richardson plots (corresponding barriers marked by O).

change their nature from conduction band to valence band states has to be aligned in both materials. A general correlation for any pair of semiconductors A and B is then deduced: $\phi_b^n(C-A) - \phi_b^n(C-B) = \Delta E_c(A-B)$, where C can be metal. In a recent paper,[11] Freeouf and Woodall argued that by using the electron affinity rule for heterojunctions[21] in conjunction with their effective work function model for Schottky barriers,[2] the abovementioned correlation is naturally expected in cases where the constituents responsible for the Fermi-level pinning in both semiconductors have similar bulk work functions. Since, in their model, this pinning constituent is usually the anion, the correlation is indeed expected for the GaAs-AlGaAs system. Since Tersoff's correlation is general for any pair of semiconductors, the correct theory can be singled out by experimentally testing a system comprised of two compound semiconductors with anions know to have different work functions (e.g., InAs-GaSb).

Assuming that the Fermi-level pinning position is doping independent,[12] we can deduce the composition dependence of $\Delta\phi_b^p$ from $\Delta\phi_b^n$,[15] as shown in Fig. 5. The values of ϕ_b^p are somewhat higher than the x dependence of the valence band discontinuity ΔE_v, measured by Batey and Wright.[19] This figure demonstrates also that the common-anion rule of McCaldin *et al.*[22] is not obeyed in the GaAs-AlGaAs system. (If it had been obeyed, $\Delta\phi_b^p$ would have been composition independent.)

IV. CARRIER TRANSPORT ACROSS THE SCHOTTKY BARRIER

A. *I-V* characteristics

We have seen in Sec. III A that at room temperature, thermionic emission dominates the transport across the Schottky barrier. Using Eq. (2) at $T = 300$ K, we found that for all Al mole fractions studied the ideality factor n (determined from the slope of log I vs V plot) was in the range between 1.1 and 1.2. For an independent determination of ϕ_b^n from J_s, the knowledge of A^* is required. Two values for A^* were used: one was determined from the Richardson plot and involved a long extrapolation of J/T^2 on a logarithmic plot to $1/T = 0$; the other was calculated assuming A^* to be proportional to m^* [the effective mass of the free carriers[15] which is given by $(0.067 + 0.083x)m_0$[23] for the free electrons in AlGaAs ($x \leqslant 0.4$)], where m_0 is the free electron mass. For $x = 0.4$, the calculated A^* increases by 50% from the widely accepted value for GaAs of 8.2–12.2 A cm^{-2} K^{-2}. Above the cross-over point, where transport is governed by the "heavy" electrons in the X valleys, A^* should be almost independent of x with a value of ~ 100 A cm^{-2} K^{-2}, assuming $m^* = (0.85 - 0.07x)\ m_0$.[23] The barrier heights calculated using the measured A^* (marked by O in Fig. 6) are identical to the activation energies obtained from the Richardson plots. For the calculated values A^*, the determined values of ϕ_b^n are marked by $\times$ in Fig. 6. The values for $x < 0.4$ are lower than the abovementioned values, while they are higher for the $x > 0.4$ regime.

The deviations from ideal thermionic emission at room temperature (reflected by $n > 1.1$) and the indications that another transport mechanism is dominant at lower temperatures (as reflected by deviations from linearity of the Richardson plots) motivated us to further study the temperature dependence of the current-voltage characteristics. This dependence (see, e.g., Fig. 3) is very similar to that already observed by Padovani and Stratton for Au on GaAs[24] and attributed to thermionic field emission (TFE). This mechanism of thermal assisted tunneling is schematically illustrated in Fig. 7. For TFE, the current-voltage relationship can be expressed by

$$I = I_s \exp(V/V_0), \tag{3}$$

where V_0 is a temperature dependent factor:

$$V_0 = E_{00} \coth(qE_{00}/kT), \tag{4}$$

and E_{00} is given by

$$E_{00} = (h/2)(N/\epsilon m^*)^{1/2}, \tag{5}$$

where ϵ is the dielectric constant and N is the free carrier concentration of the semiconductor. The pre-exponent I_s depends on T, E_{00}, ϕ_b^n, and the Fermi-level position, ξ. In principle, the barrier height can be determined from this

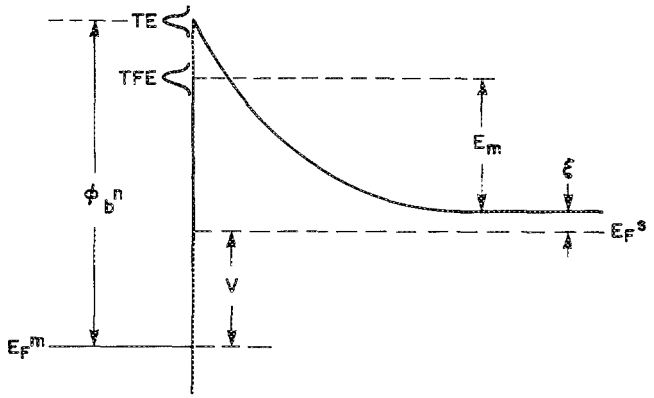

FIG. 7. Band structure at metal-semiconductor interface demonstrating thermionic emission (TE) and thermionic field emission (TFF).

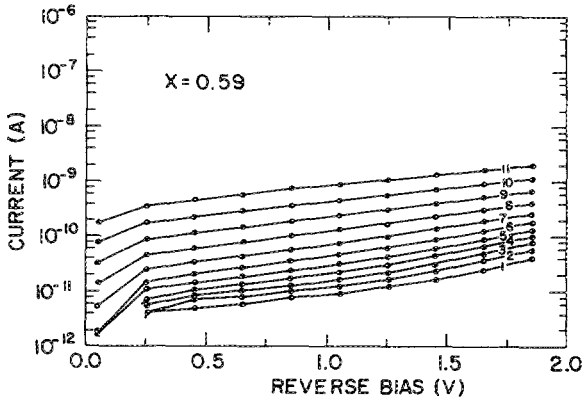

FIG. 9. Current-voltage characteristics for Schottky barriers with $x = 0.59$ under reverse biasing voltage for different temperatures: 263, 283, 298, 308, 318, 328, 338, 348, 357, 366, and 375 K (marked 1–11).

dependence; however, this involves extended extrapolations (to determine I_s at a wide range of temperatures) and leads to large inaccuracies.

In all diodes studied, it was found that the parameter V_0 monotonically increased with temperature, as expected from Eq. (4). By fitting the V_0 dependence on temperature with Eq. (4), the corresponding E_{00} was determined, as shown in Fig. 8 for $x = 0$ and $x = 0.74$. The broken line corresponds to the value of V_0 for ideal thermionic emission ($n = 1$), to which E_{00} should asymptotically reach for $kT/q \gg E_{00}$. The experimentally obtained E_{00} moderately increased with the Al mode fraction from 14 meV for $x = 0$ up to 20.4 meV for $x = 0.74$. The theoretical values according to Eq. (5) are in the range of 5–7 meV for $x < 0.4$, and 1–2 meV for $x > 0.4$. This discrepancy could be resolved only if the tunneling probability would be larger or the potential barrier narrower, as discussed in Sec. IV B.

The suggested transport mechanism of TFE is also supported by the current-voltage characteristics for reverse biasing voltage. The log I vs V plot had a linear dependence with a very moderate slope (250–1250 mV^{-1} for the different samples) for a biasing range of 0–2 V. The characteristics were almost temperature independent around 77 K, indicating a dominant tunneling current. A typical temperature dependence of some I-V curves measured at the temperature range of 263–375 K are shown in Fig. 9. For all diodes studied, the values of log I extrapolated to zero bias were somewhat higher than those obtained under forward bias (less than an order of magnitude). The Richardson plots of the reverse currents showed linear dependence of $\log I/T^2$ vs $1/T$ only at high temperatures and low biasing voltages. The activation energies, derived from the slopes of the linear region, were lower by 50–150 meV than those obtained from the corresponding curves plotted for the forward bias regime. These findings support the thermionic field emission mechanism suggested above. As the negative biasing voltage increases and the temperature decreases, the width of the potential barrier at the metal's Fermi level narrows and the tunneling current increases. The dependence of the current on the applied voltage fits the TFE model much better than any other model, such as: the image force lowering,[25] wave function penetration,[25] or generation recombination in the depletion region.[26]

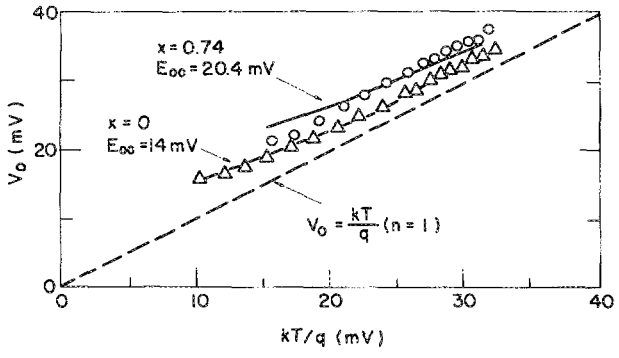

FIG. 8. V_0 values as a function of temperature for two Schottky barriers (with $x = 0$ and $x = 0.74$). For each set the best fit to Eq. (4) and the corresponding E_{00} values are marked. The broken line corresponds to an ideal case of thermionic emission.

B. Trapping centers in the AlGaAs

As discussed above, the I-V characteristics show that thermionic field emission is dominant at the low temperature range of this study; however, the use of the TFE equations indicated the existence of enhanced tunneling. Enhanced tunneling can occur if deep traps are located in the depletion layer. Using deep level transient spectroscopy (DLTS),[27] a near mid-gap level was observed in all samples. The activation energy of the trap was 0.8 eV in GaAs and was found to increase slightly as the Al mole fraction in the AlGaAs increased. The trap concentration ranged from 2×10^{15} to 2×10^{16} cm^{-3} in different samples, and there was no correlation with the Al mole fraction. The identity of these traps is unknown. A second deep trap with a thermal activation energy of 0.45 eV (independent of x) was observed in samples with $x \geqslant 0.22$. This is the so-called DX center which is responsible for the persistent photoconductivity effect in AlGaAs.[28,29] The binding energy of the DX center varies with x and is largest (0.16 eV) at $x = 0.4$.[30] The concentration of these traps was measured both by DLTS and by the photocapacitance, at 77 K. The apparent concentration[31] of the DX center increases rapidly above $x = 0.2$. It peaks near the cross-over point where the concentration is

approximately equal to the Si donor concentration, and decreases slowly thereafter as x increases.

The presence of trapping centers was suggested before to explain an observed increase in the magnitude of tunneling currents in metal-CdTe junctions.[32] A two-step process (tunneling into the traps and out) was suggested to explain the measured currents and the ideality factor of $n = 2$. Such a large n was not observed in our case, ruling out the relevance of this mechanism. A different approach was proposed by Padovani,[33] whose results for Au-GaAs barriers were similar to ours. He suggested that deep centers will alter the space-charge region, since their occupancy will be different on either side of the point at which the trap energy level crosses the Fermi level in the semiconductor. This results in a larger electric field at the interfacial region which can enhance tunneling. It is worth noting that the energy levels of the traps found in the present work seem to be either too shallow (the DX centers) or too deep (the mid-gap traps) to account for this phenomenon, according to the abovementioned model.

It should be noted that a different approach to explaining the temperature dependence of n was taken by Levine[34] and later adopted to Au-GaAs by Borrego *et al.*,[35] and more recently to Al-InP by Slowik *et al.*[36] The model is based on a finite density of surface states and a barrier whose height is controlled by the energy distribution of these states and the applied bias. No tunneling is involved in this model. Such a model may explain the variations with temperature of n for the higher temperature regime in our study, but the independence of the slopes of $\log I$ vs V on T at low temperatures is strong evidence of tunneling. It is difficult to explain the magnitude of the tunneling current for the carrier concentrations used in this work without the suggested model of narrowing the barrier potential induced by the presence of deep traps.

V. SUMMARY

The dependence of the Schottky barrier height of Mo-AlGaAs intimate junctions on the Al mole fraction was determined by the internal photoemission technique, and by activation energy plots of the current-voltage dependence on temperature. The difference between the Mo-AlGaAs barrier height (as a function of x) and Mo-GaAs was found to agree very well with the x dependence of the conduction band discontinuity in AlGaAs-GaAs heterojunctions for Al mole fraction $x < 0.4$. The measured values of $\Delta\phi_b^n$ were somewhat lower than ΔE_c for $x > 0.4$, the indirect regime; however, the general dependence on x was quite similar. If the correlation $\Delta\phi_b^n = \Delta E_c$ is indeed general, as expected from Tersoff's theoretical model, it may be used to determine ΔE_c in cases where experimental difficulties prevent a direct determination of the band discontinuity.

The temperature dependence of the current-voltage characteristics showed that for temperatures higher than 250 K, thermionic emission was the dominant transport mechanism at forward biasing voltages. The barrier heights derived from the Richardson (activation energy) plots were very similar to those obtained by the internal photoemission technique. Even in this high temperature regime, some deviations from ideal thermionic emission were observed, since $n \geqslant 1.1$ for all diodes studied. The I-V characteristics at lower temperatures were governed by thermionic field emission (thermal assisted tunneling), where enhanced tunneling currents were probably due to traps found in the AlGaAs.

ACKNOWLEDGMENTS

We thank C. Lanza and T. F. Isaacs-Smith for their help with the measurements, D. C. Thomas, I. M. Anderson, L. Osterling, and D. M. DeCain for processing the devices; and R. D. Thompson for contributions to the computer based photoemission apparatus. Useful discussions with P. M. Solomon, J. Tersoff, and Professor C. R. Crowell (USC) are gratefully acknowledged.

[1] W. Schottky, Z. Phys. **118**, 539 (1942).
[2] J. L. Freeouf and J. M. Woodall, Appl. Phys. Lett. **39**, 727 (1981).
[3] J. Bardeen, Phys. Rev. **71**, 717 (1947).
[4] V. Heine, Phys. Rev. A **138**, 1689 (1965); F. Yndurain, J. Phys. C **4**, 2849 (1971); S. G. Louie and M. L. Cohen, Phys. Rev. B **13**, 2461 (1976); C. Tejedor, F. Flores, and E. Louis, J. Phys. C **10**, 2163 (1977).
[5] J. Tersoff, Phys. Rev. Lett. **52**, 465 (1984).
[6] W. E. Spicer, P. W. Chye, P. R. Skeath, C. Y. Su, and I. Lindau, J. Vac. Sci. Technol. **16**, 1422 (1979); W. E. Spicer, I. Lindau, P. R. Skeath, C. Y. Su, and P. W. Chye, Phys. Rev. Lett. **44**, 420 (1980).
[7] J. S. Best, Appl. Phys. Lett. **34**, 522 (1979).
[8] K. Okamoto, C. E. C. Wood, and L. F. Eastman, Appl. Phys. Lett. **38**, 636 (1981).
[9] A. D. Katnani and G. Margaritondo, Phys. Rev. B **28**, 1944 (1983).
[10] J. Tersoff, J. Vac. Sci. Technol. B **3**, 1157 (1985).
[11] J. L. Freeouf and J. M. Woodall, Surf. Sci. **168**, 518 (1986).
[12] F. A. Padovani and G. G. Summer, J. Appl. Phys. **36**, 3744 (1965).
[13] J. Bloch, M. Heiblum, and Y. Komem, Appl. Phys. Lett. **46**, 1092 (1985).
[14] M. Heiblum, J. Bloch, and J. J. O'Sullivan, J. Vac. Sci. Technol. A **3**, 1885 (1985).
[15] S. M. Sze, *Physics of Semiconductor Devices* (Wiley, New York, 1981), Chap. 5.
[16] K. Kameko, M. Ayable, and N. Watanabe, Inst. Phys. Conf. Ser. No. **33a**, 216 (1977).
[17] R. C. Miller, D. A. Kleinman, and A. C. Gossard, Phys. Rev. B **29**, 7085 (1984); H. Kroemer, W. Y. Chein, J. C. Harris, and D. D. Edwall, Appl. Phys. Lett. **36**, 295 (1980); T. W. Hickmott, P. M. Solomon, R. Fischer, and M. Morkoc, J. Appl. Phys. **52**, 2844 (1984); A. Arnold, K. Keterson, T. Henderson, J. Klein, and M. Morkoc, Appl. Phys. Lett. **45**, 1237 (1984).
[18] M. Heiblum, M. I. Nathan, and M. Eizenberg, Appl. Phys. Lett. **47**, 503 (1985).
[19] J. Batey and S. Wright, J. Appl. Phys. **59**, 200 (1985).
[20] S. R. McAfee, D. V. Lang, and W. T. Tsang, Appl. Phys. Lett. **40**, 520 (1982); T. W. Hickmott, P. M. Solomon, R. Fischer, and H. Morkoc, J. Appl. Phys. **57**, 284 (1985).
[21] R. L. Anderson, Solid State Electron. **5**, 341 (1962).
[22] J. O. McCaldin, T. C. McGill, and C. A. Mead, J. Vac. Sci. Technol. **13**, 802 (1976).
[23] H. C. Casey and M. B. Panish, *Heterostructure Lasers* (Academic, New York, 1978).
[24] F. A. Padovani and R. Stratton, Solid State Electron. **9**, 695 (1966).
[25] H. K. Henisch, *Rectifying Semiconductor Contacts* (Oxford, Clarendon, London, 1957).
[26] C. T. Sah, R. N. Noyce, and W. Shockley, Proc. Inst. Radio Eng. **45**, 1228 (1957).
[27] G. L. Miller, D. V. Lang, and L. C. Kimmerling, Annu. Rev. Mater. Sci. **7**, 377 (1977).

[28]D. V. Lang, R. A. Logan, and N. Jaros, Phys. Rev. B **19**, 1015 (1979).
[29]O. Kumagi, H. Kawai, Y. Mori, and K. Kaneko, Appl. Phys. Lett. **45**, 1322 (1984).
[30]N. Chand, T. Henderson, J. Klem, W. T. Masselink, R. Fischer, Y. C. Chang, and H. Morkoc, Phys. Rev. B **30**, 4481 (1984).
[31]P. M. Mooney, N. S. Caswell, and S. L. Wright (unpublished).
[32]G. H. Parker and C. A. Mead, Phys. Rev. **184**, 780 (1969).
[33]F. A. Padovani, in *Semiconductors and Semimetals*, edited by R. K. Willardson and A. C. Beer (Academic, New York, 1971), Vol. 7a, p. 75.
[34]J. D. Levine, J. Appl. Phys. **42**, 3991 (1971).
[35]J. M. Borrego, R. J. Gutmann, and S. Ashok, Solid State Electron. **20**, 125 (1977).
[36]J. H. Slowik, H. W. Richter, and L. J. Brillson, J. Appl. Phys. **58**, 3154 (1985).